

Controlling spin Hall effect by using a band anticrossing and nonmagnetic impurity scattering

T. Mizoguchi* and N. Arakawa

Department of Physics, The University of Tokyo, 7-3-1 Hongo, Bunkyo-ku, Tokyo 113-0033, Japan

(Dated: November 6, 2018)

The spin Hall effect (SHE) is one of the promising phenomena to utilize a spin current as spintronics devices, and the theoretical understanding of its microscopic mechanism is essential to know how to control its response. Although the SHE in multiorbital systems without inversion symmetry (IS) is expected to show several characteristic properties due to cooperative roles of orbital degrees of freedom and lack of IS, the theoretical understanding of the cooperative roles has been lacked. To clarify the cooperative roles, we study the spin Hall conductivity (SHC) derived by the linear-response theory for a t_{2g} -orbital tight-binding model of the [001] surface or interface of Sr_2RuO_4 in the presence of dilute nonmagnetic impurities. We find that the band anticrossing, arising from the combination of orbital degrees of freedom and lack of IS, causes the magnitude increase and sign change of the SHC at some nonmagnetic impurity concentrations. Since the similar mechanism for controlling the magnitude and sign of the response of Hall effects works in other multiorbital systems without IS, our mechanism gives a new method to control the magnitude and sign of the response of Hall effects in some multiorbital systems by introducing IS breaking and tuning the nonmagnetic impurity concentration.

PACS numbers: 72.25.Ba, 73.40.-c, 74.70.Pq

The spin Hall effect (SHE) has been intensively studied due to its applicability to spintronics devices and theoretical interests. In the SHE, an external electric field causes the spin current (i.e., the flow of the spin angular momentum) which is perpendicular to this field^{1,2}. Since controlling a charge current is easier than controlling a spin current, the SHE has great potential for spintronics devices³. In addition, it is crucial to understand the microscopic mechanism of the SHE since it gives us a deeper understanding of how to control its response and motivates further research.

So far, we have partially understood the microscopic mechanisms of the SHE. These are categorized into intrinsic and extrinsic mechanisms: the former is related to the electronic structure⁴⁻⁸, while the latter is related to the multiple scattering of the doped impurities^{1,2,9-12}. We emphasize that the intrinsic contribution arises from not only the Berry curvature term^{4-7,13} (part of the Fermi sea term) but also the other Fermi sea term and the Fermi surface term^{8,14-16} which qualitatively differ from the Berry curvature term. In several transition metals (TMs) and TM oxides, the intrinsic mechanism is more important than the extrinsic mechanism because the intrinsic mechanism often gives a large response^{8,15} and because the extrinsic mechanism is negligible for the weak scattering potential of the doped nonmagnetic impurities. Note that the realization of such weak scattering potential is shown in a first-principle calculation in some cases¹⁷.

In general, we can understand the origin of the intrinsic SHE by detecting how an electron acquires the Aharonov-Bohm-like phase¹⁸ due to the effective flux. For that detection, it is helpful to consider the real-space motion of an electron whose first and final positions are the same because by considering that motion we can discuss a phase factor of the wave function of an electron; hereafter, we call such motion process. For example, in a multiorbital TM or TM oxide with inversion symmetry (IS)^{8,15,19-21}, the spin-dependent effective flux is generated by the process by using the z -component of the atomic spin-orbit interaction (SOI), the interorbital hopping integral between the orbitals connected by that z -component, and other hopping integrals [see Fig.

1(a)]. In addition, we can understand the SHE in the two-dimensional electron gas without IS^{5,22,23} whose electronic state is described by using the Rashba-type antisymmetric SOI²⁴ by considering the process by using the Rashba-type antisymmetric SOI and the intraorbital hopping integrals [see Fig. 1(b)].

Although there are a lot of studies about the SHE in multi-orbital systems with IS (e.g., Refs. 8 and 15) or single-orbital systems without IS (e.g., Refs. 5 and 25), we have little understood the characteristic properties of the SHE in a multiorbital system without IS. In particular, cooperative roles of orbital degrees of freedom and lack of IS have not been clarified yet, although their combination will lead to several characteristic properties of the SHE.

To clarify these roles, it is necessary to study the SHE in a multiorbital system without IS by using a model considering both orbital degrees of freedom and IS breaking correctly. It should be noted that since the combination of these leads to completely different results of several electronic properties from the results for the Rashba-type antisymmetric SOI, the correct treatment beyond the Rashba-type antisymmetric SOI is significant for multiorbital systems. Actually, the momentum dependence of the \mathbf{d} -vector of a Cooper pair completely

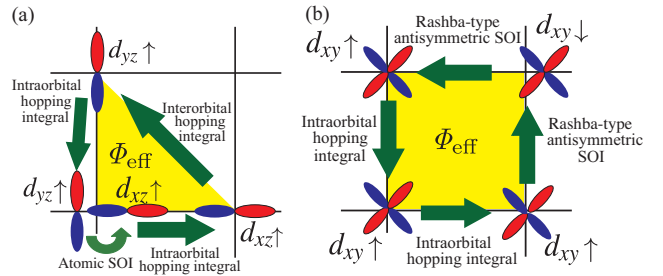


FIG. 1. (Color online) Schematic pictures of some processes generating the effective flux, Φ_{eff} , in (a) the t_{2g} -orbital model with IS⁸ and (b) the single-orbital Rashba model without IS⁵.

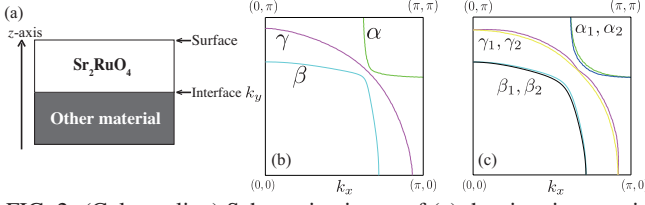


FIG. 2. (Color online) Schematic picture of (a) the situation considered, and Fermi surfaces at $t_{\text{ISB}} =$ (b) 0 and (c) 0.09 eV.

differs from that for the Rashba-type antisymmetric SOI due to the difference in the momentum dependence of the antisymmetric SOI; in the correct treatment, the antisymmetric SOI arises from the atomic SOI and the interorbital hopping integral due to the local parity mixing, induced by IS breaking^{26,27}. Since the momentum dependence of the antisymmetric SOI is important even in discussing the SHE, a study about the SHE by using the correct treatment is highly desirable.

In this Rapid Communication, we study the SHE in a t_{2g} -orbital system without IS by using the correct treatment about orbital degrees of freedom and lack of IS beyond the Rashba-type antisymmetric SOI and reveal their cooperative roles in the SHE. In particular, we find that the band anticrossing due to the cooperative roles plays an important role in controlling the magnitude and sign of the spin Hall conductivity (SHC) of a multiorbital system without IS in the presence of dilute nonmagnetic impurities. After discussing applicability of the similar mechanism, we propose the ubiquitous method to control the magnitude and sign of Hall effects by using orbital degrees of freedom, IS breaking, and nonmagnetic impurity scattering.

To discuss the SHE in a multiorbital system without IS, we consider a t_{2g} -orbital tight-binding model of the [001] surface or interface of Sr₂RuO₄ [Fig. 2(a)] in the presence of dilute nonmagnetic impurities: the Hamiltonian is $H = H_0 + H_{\text{LS}} + H_{\text{ISB}} + H_{\text{imp}}$, where $H_0 = \sum_{\mathbf{k}} \sum_{a,b} \sum_{\sigma} \varepsilon_{ab}(\mathbf{k}) c_{\mathbf{k}a\sigma}^\dagger c_{\mathbf{k}b\sigma}$, $H_{\text{LS}} = \sum_{\mathbf{k}} \sum_{a,b} \sum_{\sigma, \sigma'} \lambda [\ell \cdot \mathbf{s}]_{a\sigma b\sigma'} c_{\mathbf{k}a\sigma}^\dagger c_{\mathbf{k}b\sigma'}$, $H_{\text{ISB}} = \sum_{\mathbf{k}} \sum_{\sigma} [V_x(\mathbf{k}) c_{\mathbf{k}d_{yz}\sigma}^\dagger c_{\mathbf{k}d_{xy}\sigma} + V_y(\mathbf{k}) c_{\mathbf{k}d_{xz}\sigma}^\dagger c_{\mathbf{k}d_{xy}\sigma} + \text{H.c.}]$, and $H_{\text{imp}} = \sum_{\mathbf{k}, \mathbf{k}'} \sum_a \sum_{\sigma} v_{\text{imp}} \sum_{\mathbf{R}_j} e^{-i(\mathbf{k}-\mathbf{k}') \cdot \mathbf{R}_j} c_{\mathbf{k}a\sigma}^\dagger c_{\mathbf{k}'a\sigma}$, with $a, b = d_{yz}, d_{xz}, d_{xy}$ and $\sigma, \sigma' = \uparrow, \downarrow$. Hereafter, we set $c = \hbar = 1$ and choose the lattice constant as unity.

H_0 and H_{LS} represent the kinetic energy and atomic SOI of Sr₂RuO₄, respectively; $\varepsilon_{ab}(\mathbf{k})$ are $\varepsilon_{d_{yz}d_{yz}}(\mathbf{k}) = -2t_3 \cos k_x - 2t_2 \cos k_y - \mu$, $\varepsilon_{d_{xz}d_{xz}}(\mathbf{k}) = -2t_2 \cos k_x - 2t_3 \cos k_y - \mu$, $\varepsilon_{d_{xy}d_{xy}}(\mathbf{k}) = -2t_1 (\cos k_x + \cos k_y) - 4t_4 \cos k_x \cos k_y - \mu$, and $\varepsilon_{d_{xz}d_{yz}}(\mathbf{k}) = \varepsilon_{d_{yz}d_{xz}}(\mathbf{k}) = 4t_5 \sin k_x \sin k_y$; $[\ell \cdot \mathbf{s}]_{a\sigma b\sigma'}$ is $[\ell \cdot \mathbf{s}]_{a\sigma b\sigma'} = -\frac{1}{2}(\delta_{a,d_{yz}} \delta_{b,d_{xy}} - \delta_{b,d_{xy}} \delta_{a,d_{yz}}) \delta_{\sigma, -\sigma'} \text{sgn}(\sigma) + \frac{i}{2}(\delta_{a,d_{xz}} \delta_{b,d_{xy}} - \delta_{b,d_{xy}} \delta_{a,d_{xz}}) \delta_{\sigma, -\sigma'} \text{sgn}(\sigma) + \frac{i}{2}(\delta_{a,d_{yz}} \delta_{b,d_{xz}} - \delta_{b,d_{xz}} \delta_{a,d_{yz}}) \delta_{\sigma, \sigma'} \text{sgn}(\sigma)$ with $\text{sgn}(\sigma) = +1$ (-1) for $\sigma = \uparrow$ (\downarrow). We choose these parameters so as to reproduce the experimentally observed Fermi surface of Sr₂RuO₄²⁸: $(t_1, t_2, t_3, t_4, t_5, \lambda)$ is $(0.45, 0.675, 0.09, 0.18, 0.03, 0.045)$ (eV)²⁹ and the chemical potential, μ , is determined so that the number of electrons per a site is four.

H_{ISB} represents the interorbital hopping integral between the $d_{yz/d_{xz}}$ and d_{xy} orbitals due to the local parity mixing which

is induced by IS breaking near the [001] surface or interface^{26,27}; $V_{x/y}(\mathbf{k})$ is $V_{x/y}(\mathbf{k}) = 2it_{\text{ISB}} \sin k_{x/y}$. (For the detail of the derivation, see Supplemental material²⁷.) Note that the second-order perturbation of H_{LS} and H_{ISB} gives the Rashba-type antisymmetric SOI when the orbital degeneracy is lifted by the large crystal-electric-field energy²⁶ (see Supplemental material²⁷). In a case without IS, we set $t_{\text{ISB}} = 0.09$ eV to make t_{ISB} larger than λ and t_5 ; as we will show, this condition is essential to obtain the magnitude and sign changes of the SHC. For comparison, we also consider the case at $t_{\text{ISB}} = 0$ eV. As shown in Supplemental material²⁷, to obtain finite intrinsic SHC, only IS breaking is insufficient and finite atomic SOI is essential^{4,8}.

Diagonalizing $H_{\text{band}} = \sum_{\mathbf{k}} H_{\text{band}}(\mathbf{k}) = H_0 + H_{\text{LS}} + H_{\text{ISB}}$, we obtain the band dispersions, $E_n(\mathbf{k})$, and the unitary matrix $[U(\mathbf{k})]_{n\eta}$, where η is $\eta = (a, \sigma)$. Comparing the Fermi surfaces at $t_{\text{ISB}} = 0$, and 0.09 eV shown in Figs. 2(b), and 2(c) we see IS breaking causes the spin splitting of the α , β , and γ sheets. (At $t_{\text{ISB}} = 0$ eV, the α and β sheets are formed mainly by the d_{xz} and d_{yz} orbitals, and the γ sheet is formed mainly by the d_{xy} orbital³⁰.) In particular, the most drastic effect of IS breaking is the change of the curvature of the γ sheet around $\mathbf{k} \sim (\frac{2}{3}\pi, \frac{2}{3}\pi)$ due to the band anticrossing between the d_{xy} and $d_{xz/d_{yz}}$ orbitals. In other words, this band anticrossing causes the change of the main orbital forming the γ sheet around $\mathbf{k} \sim (\frac{2}{3}\pi, \frac{2}{3}\pi)$ from the d_{xy} orbital to the $d_{xz/d_{yz}}$ orbital. The necessary conditions for this band anticrossing are both that t_{ISB} is larger than λ and that several Fermi surface sheets whose main orbitals are connected by the transverse component of the atomic SOI are close to each other in a certain area of the Brillouin zone. H_{imp} represents the local scattering potential due to dilute nonmagnetic impurities. Assuming that the scattering is weak, we can treat its effects by the Born approximation; thus, H_{imp} affects the SHC through the self-energy correction and the current vertex correction due to the four-point vertex function^{8,15,25}. For simplicity, we assume that the main effects of H_{imp} arise from the band-independent quasiparticle damping, γ_{imp} , due to the self-energy correction, which is proportional to the nonmagnetic impurity concentration, n_{imp} . We have checked the neglected terms do not qualitatively change the results shown below³¹.

Then, we derive the SHC by the linear-response theory^{14,15}, $\sigma_{xy}^{\text{S}} = \sigma_{xy}^{\text{S(I)}} + \sigma_{xy}^{\text{S(II)}}$, where $\sigma_{xy}^{\text{S(I)}}$ is the Fermi surface term,

$$\sigma_{xy}^{\text{S(I)}} = \frac{1}{N} \sum_{\mathbf{k}} \sum_{\{\eta_1\}} \int_{-\infty}^{\infty} \frac{d\omega}{2\pi} \left(-\frac{\partial f(\omega)}{\partial \omega} \right) [j_x^{\text{S}}(\mathbf{k})]_{\eta_1 \eta_2} \times [j_y^{\text{C}}(\mathbf{k})]_{\eta_3 \eta_4} [G^{\text{R}}(\mathbf{k}, \omega)]_{\eta_2 \eta_3} [G^{\text{A}}(\mathbf{k}, \omega)]_{\eta_4 \eta_1}, \quad (1)$$

and $\sigma_{xy}^{\text{S(II)}}$ is the Fermi sea term,

$$\sigma_{xy}^{\text{S(II)}} = \frac{1}{N} \sum_{\mathbf{k}} \sum_{\{\eta_1\}} \int_{-\infty}^{\infty} \frac{d\omega}{2\pi} f(\omega) \text{Re} \left\{ [j_x^{\text{S}}(\mathbf{k})]_{\eta_1 \eta_2} [j_y^{\text{C}}(\mathbf{k})]_{\eta_3 \eta_4} \times ([G^{\text{R}}(\mathbf{k}, \omega)]_{\eta_2 \eta_3} \overleftrightarrow{\frac{\partial}{\partial \omega}} [G^{\text{R}}(\mathbf{k}, \omega)]_{\eta_4 \eta_1}) \right\}. \quad (2)$$

Here $\sum_{\{\eta_1\}}$ is $\sum_{\{\eta_1\}} \equiv \sum_{\eta_1, \eta_2, \eta_3, \eta_4}$, $f(\omega)$ is the Fermi distribution function, $f(\omega) = \frac{1}{e^{\beta\omega} + 1}$, $G^{\text{R(A)}}(\mathbf{k}, \omega)$ is the

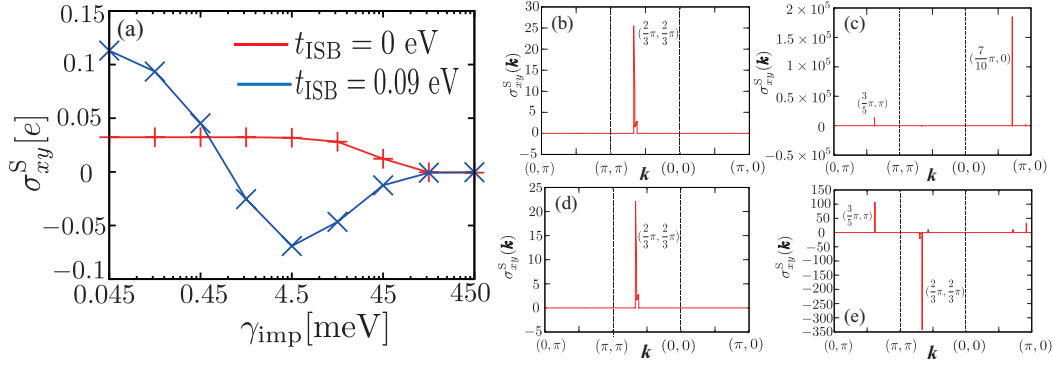


FIG. 3. (Color online) (a) γ_{imp} dependence of σ_{xy}^S at $t_{ISB} = 0$ and 0.09 eV and \mathbf{k} dependence of $\sigma_{xy}^S(\mathbf{k})$ at $(\gamma_{imp}, t_{ISB}) =$ (b) $(0.045 \text{ meV}, 0 \text{ eV})$, (c) $(0.045 \text{ meV}, 0.09 \text{ eV})$, (d) $(4.5 \text{ meV}, 0 \text{ eV})$, and (e) $(4.5 \text{ meV}, 0.09 \text{ eV})$.

retarded (advanced) Green's function, $[G^{R(A)}(\mathbf{k}, \omega)]_{\eta_1 \eta_2} = \sum_n [U^\dagger(\mathbf{k})]_{\eta_1 n} \left(\frac{1}{\omega - E_n(\mathbf{k}) + (-i)\gamma_{imp}} \right) [U(\mathbf{k})]_{n \eta_2}$, $j_y^C(\mathbf{k})$ is the charge current operator, $j_y^C(\mathbf{k}) \equiv -e \frac{\partial H_{band}(\mathbf{k})}{\partial k_y}$, $j_x^S(\mathbf{k})$ is the spin current operator, $j_x^S(\mathbf{k}) \equiv \frac{1}{2} [s_z \frac{\partial H_{band}(\mathbf{k})}{\partial k_x} + \frac{\partial H_{band}(\mathbf{k})}{\partial k_x} s_z]$, and $(g \frac{\overleftrightarrow{\partial}}{\partial \omega} h)$ is $(g \frac{\overleftrightarrow{\partial}}{\partial \omega} h) \equiv g \frac{\partial h}{\partial \omega} - \frac{\partial g}{\partial \omega} h$. It should be noted, first, that in the clean limit, where γ_{imp} satisfies $\gamma_{imp} \ll \Delta E(\mathbf{k})$ with $\Delta E(\mathbf{k})$ being the band splitting giving the dominant contribution to σ_{xy}^S , σ_{xy}^S is independent of γ_{imp} and is given mainly by the Berry curvature term, part of $\sigma_{xy}^{S(II)}$ ^{15,16}; second, that in the dirty limit, where γ_{imp} satisfies $\gamma_{imp} \gg \Delta E(\mathbf{k})$, σ_{xy}^S is proportional to γ_{imp}^{-3} and is given mainly by $\sigma_{xy}^{S(I)}$ ^{15,16}.

We turn to results, where we use 20000×20000 meshes of the first Brillouin zone because this size is necessary to suppress the finite-size effect in a clean region.

We first compare γ_{imp} dependence of σ_{xy}^S at $t_{ISB} = 0$ and 0.09 eV in Fig. 3(a). Comparing the results at $t_{ISB} = 0$ eV and 0.09 eV, we see three changes due to IS breaking: (i) an increase in a clean region ($\gamma_{imp} < 0.45$ meV), (ii) a sign change in a slightly dirty region ($0.45 \text{ meV} \leq \gamma_{imp} \leq 45 \text{ meV}$), and (iii) the appearance of a minimum at $\gamma_{imp} = 4.5$ meV. These results suggest that the magnitude and sign of σ_{xy}^S can be controlled by using orbital degrees of freedom, IS breaking, and nonmagnetic impurity scattering. As shown in Supplemental material²⁷, the above three changes hold in the different value of t_{ISB} if t_{ISB} is larger than λ and t_5 . Note, first, that in the range of γ_{imp} shown in Fig. 3(a), $\sigma_{xy}^{S(I)}$ gives the main contribution to σ_{xy}^S (see Supplemental material²⁷); second, that the residual resistivity estimated by the Drude formula is $0.1 \mu\Omega\text{cm}$ in the clean region and $0.1\text{--}10 \mu\Omega\text{cm}$ in the slightly dirty region. To clarify the origins of the above three changes, we analyze \mathbf{k} dependence of $\sigma_{xy}^S(\mathbf{k})$, defined as $\sigma_{xy}^S = \frac{1}{N} \sum_{\mathbf{k}} \sigma_{xy}^S(\mathbf{k})$, at $t_{ISB} = 0$ and 0.09 eV. From the results at $\gamma_{imp} = 0.045$ meV shown in Figs. 3(b) and 3(c), we see as t_{ISB} changes from 0 eV to 0.09 eV, the main contribution to σ_{xy}^S in the clean region changes from the region around $\mathbf{k} \sim (\frac{2}{3}\pi, \frac{2}{3}\pi)$ to the region around $\mathbf{k} \sim (\frac{7}{10}\pi, 0)$. Since the latter main contribution is larger than the former one, change (i) arises from the evolution of the larger positive-sign contribution around $\mathbf{k} \sim (\frac{7}{10}\pi, 0)$.

Then, from the results at $\gamma_{imp} = 4.5$ meV shown in Figs. 3(d) and 3(e), we see the change of t_{ISB} from 0 eV to 0.09 eV in the slightly dirty region leads to the sign-change of the main contribution to σ_{xy}^S around $\mathbf{k} \sim (\frac{2}{3}\pi, \frac{2}{3}\pi)$ from positive to negative. Thus, this sign change is the origin of change (ii). Moreover, combining the results in the clean and the slightly dirty regions, we find change (iii) arises from the competition between the opposite-sign contributions around $\mathbf{k} \sim (\frac{7}{10}\pi, 0)$ and $\mathbf{k} \sim (\frac{2}{3}\pi, \frac{2}{3}\pi)$.

In addition, to understand how each t_{2g} orbital contributes to each \mathbf{k} component of $\sigma_{xy}^S(\mathbf{k})$ at $t_{ISB} = 0$ and 0.09 eV, we analyze orbital-decomposed SHCs, obtained by the equations that the summations with respect to orbital and spin indices in Eqs. (1) and (2) are restricted.

Before the results at $t_{ISB} = 0.09$ eV, we explain the relation between the main \mathbf{k} component of $\sigma_{xy}^S(\mathbf{k})$ and each t_{2g} orbital at $t_{ISB} = 0$ eV. Considering all the possible orbital-decomposed SHCs which give the finite contribution to σ_{xy}^S and calculating these values, we find that in the clean and the slightly dirty regions, the main contribution to σ_{xy}^S arises from the term containing $[j_x^S(\mathbf{k})]_{d_{xz}\sigma d_{xz}\sigma} [j_y^C(\mathbf{k})]_{d_{yz}\sigma d_{yz}\sigma}$ around $\mathbf{k} \sim (\frac{2}{3}\pi, \frac{2}{3}\pi)$ near the Fermi level; that main contribution arises from the process shown in Fig. 4(a). Although the process shown in Fig. 1(a) contributes to that term, this contribution is smaller than the above contribution [i.e., Fig. 4(a)] in the clean and the slightly dirty regions since the ratio of the magnitude of the former to the latter is roughly proportional to γ_{imp}/λ [see Eqs. (6) and (7) in Ref. 8]. Thus, all the t_{2g} orbitals around $\mathbf{k} \sim (\frac{2}{3}\pi, \frac{2}{3}\pi)$ near the Fermi level play an important role in the SHE at $t_{ISB} = 0$ eV.

We go on to explain the relation at $t_{ISB} = 0.09$ eV. By using the similar analysis, we find in the clean region, the main contribution to σ_{xy}^S arises from the term containing $[j_x^S(\mathbf{k})]_{d_{xz}\sigma d_{xz}\sigma} [j_y^C(\mathbf{k})]_{d_{xz}\sigma' d_{xy}\sigma'}$ or $[j_x^S(\mathbf{k})]_{d_{xz}\sigma d_{xz}\sigma} [j_y^C(\mathbf{k})]_{d_{xy}\sigma' d_{xz}\sigma'}$ around $\mathbf{k} \sim (\frac{7}{10}\pi, 0)$ near the Fermi level, whose main contribution arises from the process shown in Fig. 4(b). We also find in the slightly dirty region, the main contribution to σ_{xy}^S arises from the term containing $[j_x^S(\mathbf{k})]_{d_{xz}\sigma d_{xz}\sigma} [j_y^C(\mathbf{k})]_{d_{yz}\sigma d_{yz}\sigma}$ around $\mathbf{k} \sim (\frac{2}{3}\pi, \frac{2}{3}\pi)$ near the Fermi level, whose main contribution arises from the process

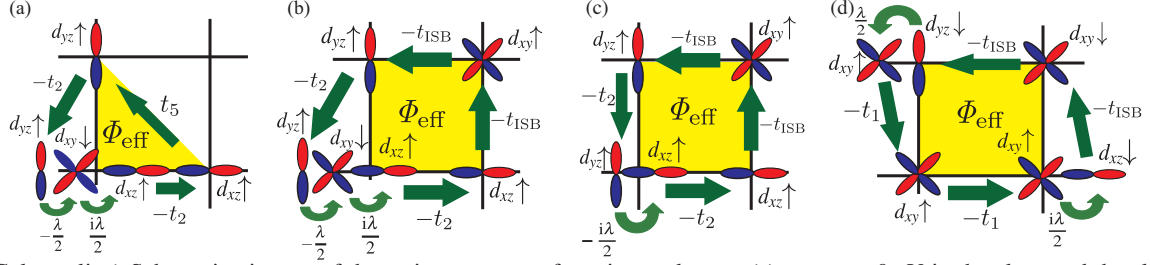


FIG. 4. (Color online) Schematic pictures of the main processes of a spin-up electron (a) at $t_{\text{ISB}} = 0$ eV in the clean and the slightly dirty region, and at $t_{\text{ISB}} = 0.09$ eV in (b) the clean and (c) the slightly dirty region, and of (d) an extended Rashba-type process.

shown in Fig. 4(c). We should note, first, that these processes can be regarded as not the extended Rashba-type ones but the characteristic ones of a multiorbital system without IS since these completely differ from the extended Rashba-type process such as Fig. 4(d); second, that in the slightly dirty region, although the contribution arising from the process shown in Fig. 4(a) is opposite sign against the main contribution [i.e., Fig. 4(c)], the former is smaller due to $t_{\text{ISB}} > t_5$ and $t_{\text{ISB}} > \lambda$. Thus, all the t_{2g} orbitals around $\mathbf{k} \sim (\frac{7}{10}\pi, 0)$ and $(\frac{2}{3}\pi, \frac{2}{3}\pi)$, affected by the spin splitting due to IS breaking, near the Fermi level become important in the SHE at $t_{\text{ISB}} = 0.09$ eV. In particular, the sign change of the contribution around $\mathbf{k} \sim (\frac{2}{3}\pi, \frac{2}{3}\pi)$ due to the band anticrossing and its competition with the opposite-sign contribution around $\mathbf{k} \sim (\frac{7}{10}\pi, 0)$ are vital to obtain the magnitude and sign change of the SHC as a function of γ_{imp} .

We emphasize that our mechanism for controlling the magnitude and sign of the SHC is new and qualitatively different from the mechanism proposed in the single-orbital model³² with the Rashba-type and Dresselhaus-type³³ antisymmetric SOI. This is because our mechanism does not need the bulk IS breaking which is necessary to obtain the Dresselhaus-type antisymmetric SOI.

We now discuss applicability of our mechanism for controlling the magnitude and sign of the SHC to other systems. If the following three conditions are satisfied, we can control the magnitude and sign of the SHC in a multiorbital system by introducing IS breaking and tuning n_{imp} . These conditions are, first, that there are several (at least two) same-sign contributions from $\sigma_{xy}^S(\mathbf{k})$ at some momenta in a case without IS in the absence of the band anticrossing; second, that the band anticrossing occurs at one of these momenta due to the combination of orbital degrees of freedom and IS breaking; third, that the value of the band splitting at momentum where the band anticrossing occurs differs from the values of the band splittings giving the other contributions. If the first and second conditions are satisfied, we have the different-sign components of $\sigma_{xy}^S(\mathbf{k})$ at some momenta since the band anticrossing causes the sign change of $\sigma_{xy}^S(\mathbf{k})$ at one of these momenta as a result of the change of the main orbital of the Fermi surface sheet. In addition, if the third condition is satisfied, we can control the magnitude and sign of $\sigma_{xy}^S(\mathbf{k})$ by

tuning the value of γ_{imp} through n_{imp} since an increase of γ_{imp} causes a larger decrease of the contribution of $\sigma_{xy}^S(\mathbf{k})$ arising from $\Delta E_1(\mathbf{k})$ than a decrease of the contribution of $\sigma_{xy}^S(\mathbf{k})$ arising from $\Delta E_2(\mathbf{k}) > \Delta E_1(\mathbf{k})$, $;\Delta E_1(\mathbf{k})$ [$\Delta E_2(\mathbf{k})$] is the band gap at the momentum from which the negative [positive] contribution comes. Since a large value of t_{ISB} is necessary for the band anticrossing and an increase of the potential of the local parity mixing due to IS breaking enhances t_{ISB} , these three conditions can be realized even in other multiorbital systems by introducing IS breaking and tuning n_{imp} . The surface of SrTiO_3 ^{34,35} and the interface between SrTiO_3 and LaAlO_3 ³⁶⁻³⁸ may be the good candidates.

Moreover, the similar mechanism is applicable to other Hall effects such as the anomalous Hall effect^{16,39} since the band anticrossing due to the combination of orbital degrees of freedom and IS breaking drastically affects the main process(es) generating the effective flux.

Thus, our mechanism gives a ubiquitous method to control the magnitude and sign of the response of Hall effects in multiorbital systems without IS.

In summary, we studied the SHE in the t_{2g} -orbital tight-binding model of the [001] surface or interface of Sr_2RuO_4 in the presence of dilute nonmagnetic impurities on the basis of the linear-response theory. We found that the SHC shows the magnitude increase and sign change as a function of γ_{imp} when the band anticrossing occurs at $\mathbf{k} = (\frac{2}{3}\pi, \frac{2}{3}\pi)$ due to the cooperative roles of orbital degrees of freedom and IS breaking and its contribution to the SHC becomes dominant compared with the contributions from $\sigma_{xy}^S(\mathbf{k})$ at the other momenta by increasing γ_{imp} . Since the similar situation can be realized in other systems by tuning the potential of the local parity mixing due to IS breaking and n_{imp} , we propose that the magnitude and sign of the response of Hall effects in some multiorbital systems can be controlled by introducing IS breaking and tuning n_{imp} .

ACKNOWLEDGMENTS

We would like to thank M. Ogata, S. Murakami, and T. Okamoto for fruitful discussions and comments.

- * mizoguchi@hosi.phys.s.u-tokyo.ac.jp
- ¹ M. I. Dyakonov, and V. I. Perel, *Sov. Phys. JETP Lett.* **13**, 467 (1971); M. I. Dyakonov, and V. I. Perel, *Phys. Lett.* **A35**, 459 (1971).
 - ² J. E. Hirsch, *Phys. Rev. Lett.* **83**, 1834 (1999).
 - ³ S. A. Wolf, D. D. Awschalom, R. A. Buhrman, J. M. Daughton, S. von Molnár, M. L. Roukes, A. Y. Chtchelkanova, and D. M. Treger, *Science* **294**, 1488 (2001).
 - ⁴ S. Murakami, N. Nagaosa, and S. C. Zhang, *Science* **301**, 1348 (2003).
 - ⁵ J. Sinova, D. Culcer, Q. Niu, N. A. Sinitsyn, T. Jungwirth, and A. H. MacDonald, *Phys. Rev. Lett.* **92**, 126603 (2004).
 - ⁶ S. Murakami, N. Nagaosa, and S. C. Zhang, *Phys. Rev. Lett.* **93**, 156804 (2004).
 - ⁷ C. L. Kane, and E. J. Mele, *Phys. Rev. Lett.* **95**, 226801 (2005).
 - ⁸ H. Kontani, T. Tanaka, D. S. Hirashima, K. Yamada, and J. Inoue, *Phys. Rev. Lett.* **100**, 096601 (2008).
 - ⁹ J. Smit, *Physica* **24**, 39 (1958).
 - ¹⁰ L. Berger, *Phys. Rev. B* **2**, 4559 (1970).
 - ¹¹ A. Crépieux, and P. Bruno, *Phys. Rev. B* **64**, 014416 (2001).
 - ¹² S. Pandey, H. Kontani, D. S. Hirashima, R. Arita, and H. Aoki, *Phys. Rev. B* **86**, 060507 (R) (2012).
 - ¹³ M. Onoda, and N. Nagaosa, *J. Phys. Soc. Jpn.* **71**, 19 (2002).
 - ¹⁴ P. Středa, *J. Phys. C: Solid State Phys.* **15**, L717 (1982).
 - ¹⁵ T. Tanaka, H. Kontani, M. Naito, T. Naito, D. S. Hirashima, K. Yamada, and J. Inoue, *Phys. Rev. B* **77**, 165117 (2008).
 - ¹⁶ H. Kontani, T. Tanaka, and K. Yamada, *Phys. Rev. B* **75**, 184416 (2007).
 - ¹⁷ K. Nakamura, R. Arita, and H. Ikeda, *Phys. Rev. B* **83**, 144512 (2011).
 - ¹⁸ See, e.g., J. J. Sakurai, *Modern Quantum Mechanics* (Benjamin/Cummings, Menlo Park, CA, 1985).
 - ¹⁹ E. Saitoh, M. Ueda, H. Miyajima, and G. Tatara, *Appl. Phys. Lett.* **88**, 182509 (2006).
 - ²⁰ T. Kimura, Y. Otani, T. Sato, S. Takahashi, and S. Maekawa, *Phys. Rev. Lett.* **98**, 156601 (2007).
 - ²¹ M. Morota, Y. Niimi, K. Ohnishi, D. H. Wei, T. Tanaka, H. Kontani, T. Kimura, and Y. Otani, *Phys. Rev. B* **83**, 174405 (2011).
 - ²² Y. K. Kato, R. C. Myers, A. C. Gossard, and D. D. Awschalom, *Science* **306**, 1910 (2004).
 - ²³ J. Wunderlich, B. Kaestner, J. Sinova, and T. Jungwirth, *Phys. Rev. Lett.* **94**, 047204 (2005).
 - ²⁴ E. I. Rashba, *Sov. Phys. Solid State* **2**, 1109 (1960).
 - ²⁵ J. Inoue, G. E. W. Bauer, and L. W. Molenkamp, *Phys. Rev. B* **67**, 033104 (2003).
 - ²⁶ Y. Yanase, *J. Phys. Soc. Jpn.* **82**, 044711 (2013).
 - ²⁷ Supplemental material.
 - ²⁸ A. P. Mackenzie, S. R. Julian, A. J. Diver, G. J. McMullan, M. P. Ray, G. G. Lonzarich, Y. Maeno, S. Nishizaki, and T. Fujita, *Phys. Rev. Lett.* **76**, 3786 (1996).
 - ²⁹ N. Arakawa, and M. Ogata, *Phys. Rev. B* **87**, 195110 (2013).
 - ³⁰ I. I. Mazin, and D. J. Singh, *Phys. Rev. Lett.* **79**, 733 (1997).
 - ³¹ T. Mizoguchi, and N. Arakawa, in preparation.
 - ³² N. A. Sinitsyn, E. M. Hankiewicz, W. Teizer, and J. Sinova, *Phys. Rev. B* **70**, 081312 (R) (2004).
 - ³³ G. Dresselhaus, *Phys. Rev.* **100**, 580 (1955).
 - ³⁴ K. Ueno, S. Nakamura, H. Shimotani, A. Ohtomo, N. Kimura, T. Nojima, H. Aoki, Y. Iwasa, and M. Kawasaki, *Nat. Mater.* **7**, 855 (2008).
 - ³⁵ P. D. C. King, S. McKeown Walker, A. Tamai, A. de la Torre, T. Eknapakul, P. Buaphet, S.-K. Mo, W. Meevasana, M. S. Bahramy, and F. Baumberger, *Nat. Commun.* **5**, 3414 (2014).
 - ³⁶ A. Ohtomo, and H. Y. Hwang, *Nature* **427**, 423 (2004).
 - ³⁷ M. Hirayama, T. Miyake, and M. Imada, *J. Phys. Soc. Jpn.* **81**, 084708 (2012).
 - ³⁸ Y. Nakamura, and Y. Yanase, *J. Phys. Soc. Jpn.* **82**, 083705 (2013).
 - ³⁹ R. Karplus, and J. M. Luttinger, *Phys. Rev.* **95**, 1154 (1954); J. M. Luttinger, *Phys. Rev.* **112**, 739 (1958).